Performance Analysis for DF Relay-Aided Visible Light Communication System With NOMA

Manjing Zhu, *Graduate Student Member, IEEE*, Yuhao Wang , *Senior Member, IEEE*,
Xiaodong Liu , *Member, IEEE*, Shuai Ma , *Member, IEEE*, Xun Zhang , *Senior Member, IEEE*,
and Yaru Fu, *Member, IEEE*

Abstract—**Visible light communication (VLC) has been deemed to be one promising technique for the sixth-generation wireless communication network. However, due to the attenuation properties, the VLC ranges are usually limited. To unlock the advantage of multiple light-emitting diodes (LEDs) and extend the coverage of VLC systems, a relay-aided VLC system with non-orthogonal multiple access (NOMA) is proposed in this paper. Specifically, a decode-and-forward (DF) relay protocol is introduced to construct the relay-aided VLC system with NOMA. Moreover, the closed-form expression of the outage probability (OP) in the DF relay-aided VLC system with NOMA is derived to accurately characterize the theoretical performance of the system. Thereafter, the effects of the corresponding parameters on the OP are investigated. Simulation results verify the accuracy of the derived theoretical expression and illustrate that the DF relay-aided VLC system with NOMA can effectively improve system outage performance. Compared to the direct transmission NOMA VLC system without relay link, our scheme can obtain 15 dB transmit signal-to-noise ratio gains in 10^{-3} OP level. Last but not least, the optimal transmit semi-angle and deployment height of the relay can be determined for achieving the optimal system outage performance.**

Index Terms—**Visible light communication, non-orthogonal multiple access, outage probability, relay, decode-and-forward.**

Manjing Zhu is with the School of Information Engineering, Nanchang University, Nanchang 330031, China, and also with the Modern Education Technology Center, Jiangxi Open University, Nanchang 330046, China (e-mail: zhumanjing@jxrtvu.com).

Yuhao Wang is with the School of Information Engineering, Nanchang University, Nanchang 330031, China, and also with Shangrao Normal College, Shangrao 334001, China (e-mail: wangyuhao@ncu.edu.cn).

Xiaodong Liu is with the School of Information Engineering, Nanchang University, Nanchang 330031, China (e-mail: xiaodongliu@whu.edu.cn).

Shuai Ma is with the Shanxi Key Laboratory of Information Communication Network and Security, Xi'an University of Posts and Telecommunications, Xi'an 710121, China, and also with National Mobile Communications Research Laboratory, Southeast University, Nanjing 211189, China (e-mail: mashuai001@cumt.edu.cn).

Xun Zhang is with the Institut Suprieur d'Electronique de Paris, ISEP, 92130 Paris, France (e-mail: xun.zhang@isep.fr).

Yaru Fu is with the School of Science and Technology, Hong Kong Metropolitan University, Hong Kong 999077, China (e-mail: yfu@hkmu.edu.hk).

Digital Object Identifier 10.1109/JPHOT.2022.3204687

I. INTRODUCTION

THE spectrum shortage problem of radio frequency (RF) wireless communication networks becomes more and more serious with the ever-increasing wireless mobile devices and unprecedented communication data service demands [1], [2]. Fortunately, due to the license-free and rich visible light spectrum resources from 380 nm to 780 nm as well as its effective frequency and spatial reuse, visible light communication (VLC) has been deemed to be an indispensable supplement technology to relieve spectrum resource scarcity, and it has drawn an increasing attention from both academia and industry [3]. More importantly, it can simultaneously provide illumination and high-data rate communication services [4]. Furthermore, VLC has several significant advantages, such as high energy efficiency, high security, being immunity to electromagnetic interference, health friendly and low cost [5].

Although the propagation characteristic of visible light brings reuse and security gains of the VLC systems, the transmission range and coverage of visible light are limited and the influence of shadows or obstacles cannot be ignored [6]. In particular, the transmission rates of the users which located at the service region edge of VLC systems are usually lower and even occur outage [7]. Thus, it is a significant challenge to alleviate the channel degradation and improve the quality of service (QoS) of the cell-edge users with the absence of a strong direct link.

Cooperative relay is an efficient technique in improving system connectivity and extending the coverage in RF communications [8]. Moreover, there are multiple light-emitting diode (LED) illuminators with different configurations and deployment heights in an indoor scenario to satisfy different lighting scenario demands. Thus, it is interesting introducing the cooperative relay terminals into VLC scenario to improve the overall throughput and communication coverage of VLC systems. Based on the motivation, there are numerous works focused on orthogonal multiple access (OMA)-based VLC systems by using relay terminals to improve the system reliability performance [9], [10], [11]. Specifically, the authors in [11] proposed a relay-aided VLC system based on asymmetrically clipped direct current (DC) biased optical orthogonal frequency division multiplexing and derived the expression of throughput. Moreover, the optimal power allocation factor of the relay is

investigated to achieve the maximum throughput performance. Nevertheless, those research results of focusing on the performance of OMA-based VLC systems show that the system spectrum is underutilized.

To simultaneously enhance spectral efficiency and user fairness, non-orthogonal multiple access (NOMA) has been proposed as a prospective technique to apply into VLC systems [12], [13]. Different from the OMA strategy, NOMA enables multiple users to coexist on the same time-frequency resource [14], [15]. The main idea behind NOMA is that the transmitter combines multi-user signals together by adopting the superposition coding in the power domain and the receiver separates these superimposed signals by using the successive interference cancellation (SIC) technology [16], [17]. In this coding process, more power is allocated to the users with poor channel quality and the users with good channel quality are allocated less power. Correspondingly, the user with more allocated power is decoded and removed firstly in the SIC process. In [18], the user with a better channel condition acts as a relay after decoding the message for the user with a poor channel condition by using SIC technology. Therefore, NOMA can achieve a larger information theoretic rate region and can provide a higher fairness service [19], [20]. Moreover, the performance gain achieved by NOMA is more prominent in the case of high signal-to-noise ratio (SNR) scenarios [21]. In addition, VLC systems can easily provide high SNRs due to the short transmission distance with the dominant line-of-sight (LoS) links in the VLC channel. Thus, the integration of NOMA and VLC systems can effectively improve spectral efficiency, the fairness of users and system performance [22], [23]. In [22], a NOMA VLC system was proposed and the closed-form expressions of both two users' outage probability (OP) and ergodic sum rate were derived in a downlink VLC network. It also showed that NOMA could offer a higher performance gain compared with OMA. In [23], the bit error rate (BER) and achievable rate performance of cooperative NOMA VLC system under perfect CSI was analyzed, and it showed that cooperative NOMA outperformed non-cooperative NOMA by 8.2 dB at 10^{-6} BER level in a two-user scenario.

In order to extend the transmission range of NOMA VLC systems, there are some works focusing on VLC systems based on cooperative NOMA and hybrid VLC/RF link [24]-[26]. In [24], the authors proposed a cross-band selection combining (CBSC) method for a two-user hybrid lightwave/RF cooperative networks with NOMA. According to CBSC, the far user adaptively chooses either the mixed VLC/RF relaying link or the direct VLC link to decode the information. In [25], a simultaneous lightwave information and power transfer-based dual-hop hybrid VLC/RF cooperative communication system was proposed, and the closed-form expression of the end-to-end OP was obtained. The relay terminal in hybrid VLC/RF systems can extend the transmission range of VLC systems, but the relay terminal is in practice operated in RF communication link while not in VLC link [26]. Note that the RF link requires authorization and the hybrid VLC/RF systems have higher demands on transceivers. Thus, it is attractive to investigate the pure VLC relay link with NOMA.

However, it faces a significant challenge to investigate the relay-aided VLC system with NOMA. Those results in [24]-[26] are not suitable for the relay-aided NOMA-based VLC scenarios. They cannot be directly applied to the relay-assisted VLC systems with NOMA since the VLC channel mode is different from RF communication link. More particularly, in a practical VLC system, the transmission signal must be satisfied to the requirement of the non-negativity real value and the constraints on peak amplitude and average power [27]. Thus, the corresponding channel capacity is different from the classic Shannon capacity. Moreover, the interference among NOMA users obviously affects the receiver decoding process and complicates the system design.

In addition, amplify-and-forward (AF) relaying also amplifies noise when amplifying signals, it decreases the SNR and deteriorates the systems performance. The authors in [9], [28] and [29] proved that the performance of decode-and-forward (DF) relaying system outperformed that of AF relaying system. In [9], the authors have proved that DF relaying provided higher BER performance gain over AF relaying in the VLC system based on OMA. In [28], the authors have proved that in the RF communication system, NOMA-DF always outperformed NOMA-AF in terms of ergodic sum rate, and NOMA-DF exhibited a better outage behavior than NOMA-AF at low SNR. The simulation results in [29] also demonstrated DF relaying obtained a higher secrecy rate over AF relaying in the VLC system. In order to focus on investigating the relay performance and the influences of the corresponding LED parameters in the NOMA-VLC systems, the DF relay protocol is directly introduced in this paper. Recognizing these criticisms, it is of high necessity to study the DF relay-aided VLC system with NOMA.

Motivated by those facts, a DF relay-aided VLC system with NOMA is considered in this paper. Moreover, the system outage performance and corresponding impact factors are investigated. Different from the works in [24]-[26], the main contributions of this paper are summarized as follows.

1) In the proposed DF relay-aided VLC system with NOMA, the relay terminal is operated in VLC link. Moreover, we unlock this natural advantage of multiple LEDs with different configurations and deployment heights in an indoor scenario by choosing a LED closest to the cell-edge users as the cooperative relay. In addition, the fairness of cell-edge users has been improved by the combination of the relay and NOMA.

2) In order to provide meaningful insight into the considered DF relay-aided VLC system with NOMA, the practical peak amplitude and average power constraints are considered and a tight lower bound of the achievable rate for VLC systems is adopted to analyze the system outage performance. Then, the probability density function (PDF) and the corresponding cumulative distribution function (CDF) of the VLC ordered channel gain is firstly derived based on the statistical probability scheme to describe the characteristics of randomly distributed users. Therefore, the analyzed closed-form expression of the OP is obtained
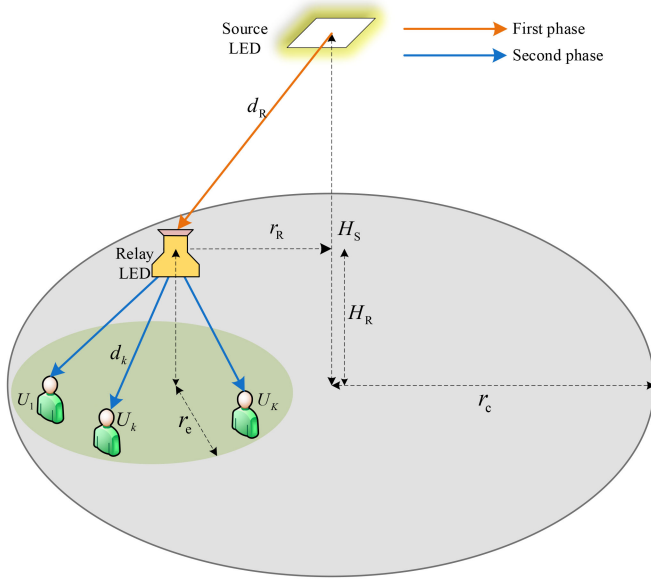
Fig. 1. Relay-aided NOMA VLC system model.

based on the CDF of channel gain and the lower bound of the user achievable rate.

3) Simulation results verify the accuracy of the derived theoretical expression. Moreover, the simulation results show the proposed DF relay-aided VLC system with NOMA can effectively improve the system outage performance. Compared to the direct transmission (DT) NOMA VLC system without relay link, the proposed scheme can obtain 15 dB transmit SNR gains in 10^{-3} OP level. Furthermore, the corresponding impact factors of the system outage performance are investigated from relay transmit semi-angle, relay deployment height, relay radiation radius and power allocation factor. The optimal relay transmit semi-angle and relay deployment height can be obtained to achieve the minimum OP. These optimal parameters can effectively guide the deployment of relay networks.

The rest of this paper is organized as follows. The system model and relay transmission process are introduced in Section II. Section III analyzes distribution function of the VLC channel and the system outage performance. Simulation results are presented and discussed in Section IV. Finally, conclusions are drawn in Section V.

II. SYSTEM MODEL

The considered indoor downlink DF relay-aided VLC system with NOMA model is shown in Fig. 1, a source LED transmitter is located at the center of the ceiling with a height of H_S from the floor, which is considered as the main node to access the backbone network. The source LED simultaneously provide illumination and communication services for all users distributed within the radiation area of maximum radius r_c. Due to the VLC channel attenuation, the direct link between source LED and the cell-edge users is usually poor or even absent in the VLC system [11]. In order to improve QoS of the cell-edge users,

we focus on the transmission between the source LED and the cell-edge users in this paper.

A LED task light closest to K cell-edge users $\{U_1, \ldots, U_k, \ldots U_K\}$ is chosen as the cooperative relay, which is located at a horizontal distance r_R from the center of the cell and a vertical distance H_R from the floor and has a maximum radiation radius r_e for K cell-edge users services. The cell-edge K users are uniformly distributed in the cell-edge area of radius r_e radiated by the relay. Specifically, the relay has a receiver photodiode (PD) and a transmitter LED, namely, it can receive signals with the PD and transmit signals with the LED. Thus, the relay is called as relay LED-PD. Note that the system is suitable for Internet-of-Thing (IoT) network scenarios composed of multiple sensors. The relay LED-PD operates in a half-duplex mode. The signal transmission process between the source LED and cell-edge users follows that relay LED-PD firstly receives signal from the source LED and then decodes signal and forwards to cell-edge users with NOMA. Therefore, the communication process between the source LED and the cell-edge users contains two phases which are source LED transmission and relay LED-PD forwarding.

In VLC systems, the VLC channels are dominated by the LoS link [30]. Similar to [15] and [22], only the LoS link is considered in this paper. Thus, based on LED Lambertian emission pattern, both the channel gain h_{SR} and h_{RU_k} can be generally modeled as [30]

$$h_\Omega = \frac{(m+1)A_\Omega R_{PD} \cos\varphi}{2\pi d_\Omega^2} \cos^m(\theta) g(\varphi) T(\varphi), \quad (1)$$

where $\Omega \in \{SR, RU_k\}$, subscript SR represents the channel link between source LED and relay LED-PD, subscript RU_k denotes the channel link between relay LED-PD and the k-th cell-edge user. A_Ω and d_Ω represent the detection area of the PD device and the Euclidean distance for the channel link of the Ω, respectively. R_{PD} denotes the PD responsivity. m is the Lambertian emission order and can be calculated by $m = -\ln(2)/\ln(\cos\phi_{1/2})$, $\phi_{1/2}$ denotes the semi-angle of the LED [26]. φ and θ represent the incident and radiation angle, respectively. $g(\varphi) = n^2/\sin^2(\Psi), (0 \le \varphi \le \Psi)$, is the optical concentrator (OC) gain and depends on the refractive index n of the OC and the field of view (FoV) Ψ of the PD [30]. $T(\varphi)$ is the optical filter gain. Note that $h_\Omega = 0$ when $\varphi > \Psi$. $\phi_{1/2}$, φ, and θ of both source LED and relay LED-PD are assumed to be the same, respectively. Moreover, without loss of generality [22], it is assumed that the channel condition of the first user is the worst and the channel condition of the K-th user is best in the DF relay-aided VLC system with NOMA. The channel gains between relay LED-PD and K users are assumed to be ordered with $h_{RU_1} \le \cdots \le h_{RU_k} \le \cdots \le h_{RU_K}$.

A. Source LED Transmission

In the first phase, source LED broadcasts K users' superposed signals to relay LED-PD based on the power domain NOMA principle. The signal transmitted from the source LED is given

by

$$x_{\mathrm{S}} = \sum_{k=1}^{K} \sqrt{\alpha_k P_{\mathrm{ST}}} s_k + I_{\mathrm{DC}}, \tag{2}$$

where subscript S denotes source LED, P_{ST} and α_k are the total transmission power of source LED and the power allocation coefficient for the k-th user which is subject to the constraint $\sum_{k=1}^{K} \alpha_k = 1$, respectively. s_k represents the desired signal for the k-th user, which is assumed to be zero-mean with unit variance and is subject to amplitude constraint, and is expressed as $|s_k| \leq \mathcal{A}$, where $\mathcal{A} > 0$ is a constant [15]. $I_{\mathrm{DC}} \in [I_L, I_H]$ is DC bias offset added to source LED to satisfy the non-negative requirement of transmission signals in VLC systems, and the corresponding I_L and I_H are the minimum and maximum input DC bias offset in LED linear region, respectively. To guarantee the transmitted signal be non-negative, it must be satisfied to $\mathcal{A} \leq I_{\mathrm{DC}}$ [15]. In order to avoid harmonic distortion by the nonlinearity of the LED, the signal input to the LED must be restrained within the linear region of the LED operation [31]. Thus, $\mathcal{A}$ must be satisfied to

$$\mathcal{A} \leq \min\left(I_{\mathrm{DC}} - I_{\mathrm{L}}, I_{\mathrm{H}} - I_{\mathrm{DC}}\right). \tag{3}$$

According to (2), the average optical power of the transmitted signal x is given by

$$P_{\mathrm{a}} = \mathbb{E}\left\{ \sum_{k=1}^{K} \sqrt{\alpha_k P_{\mathrm{ST}}} s_k + I_{\mathrm{DC}} \right\} = I_{\mathrm{DC}}. \tag{4}$$

Based on the NOMA principle, users with poorer channel gain are allocated more power. Thus, the power allocation coefficient follows $\alpha_1 \geq \cdots \geq \alpha_k \geq \cdots \geq \alpha_K$. The received signal of the relay LED-PD after removing the DC component is given by

$$y_{\mathrm{SR}} = \underbrace{h_{\mathrm{SR}} \sqrt{\alpha_k P_{\mathrm{ST}}} s_k}_{\text{desired signal}} + \underbrace{h_{\mathrm{SR}} \sum_{i=1,i\neq k}^{K} \sqrt{\alpha_i P_{\mathrm{ST}}} s_i}_{\text{multiuser interererence}} + n_{\mathrm{SR}}, \tag{5}$$

where $n_{\mathrm{SR}} \sim \mathcal{N}(0, \sigma_{\mathrm{SR}}^2)$ denotes the additive white Gaussian noise in the channel link SR, and σ_{SR}^2 is the corresponding noise power. The second item in (5) is the multiuser interference caused by non-orthogonal transmission. Based on the NOMA principle, the SIC is applied to eliminate the interference with the weaker channel gains, namely, the channel gain of $h_i, (i < k)$ is removed.

B. Relay LED-PD Forwarding

In DF relaying transmission process, relay LED-PD firstly decodes the desired signal for all users by the SIC, and then transmits the reconstructed superposition signal for all cell-edge users. Note that the signal transmitted by relay LED-PD is different from the signal transmitted by source LED. The signal transmitted by the relay LED-PD is

$$x_{\mathrm{R}} = \sum_{k=1}^{K} \sqrt{\beta_k P_{\mathrm{RT}}} s_k' + I_{\mathrm{DC}}', \tag{6}$$

where subscript R denotes relay LED-PD. s_k' denotes the signal decoded by the relay LED-PD, similar to s_k, $|s_k'| \leq \mathcal{A}$. β_k

denotes the power allocation coefficient for the k-th user in the DF relaying transmission process, which is subject to the constraint $\sum_{k=1}^{K} \beta_k = 1$. Similar to α_k, β_k follows $\beta_1 \geq \cdots \geq \beta_k \geq \cdots \geq \beta_K$. P_{RT} is the transmit power of relay LED-PD and is satisfied to the requirement of the minimum forwarded power. $I_{\mathrm{DC}}' \in [I_L, I_H]$ is DC bias offset added to relay LED-PD to satisfy the non-negative requirement of transmission signals in VLC systems. Taking into account the very limited delay in the proposed system, similar to [32], the delay in the proposed system can be ignored. Therefore, the received signal of the k-th user after removing the DC component is given by

$$y_{\mathrm{RU}_k} = \underbrace{h_{\mathrm{RU}_k} \sqrt{\beta_k P_{\mathrm{RT}}} s_k'}_{\text{desired signal}} + \underbrace{h_{\mathrm{RU}_k} \sum_{i=1,i\neq k}^{K} \sqrt{\beta_i P_{\mathrm{RT}}} s_i'}_{\text{multiuser interference}} + n_{\mathrm{RU}_k},$$
$$\tag{7}$$

where $n_{\mathrm{RU}_k} \sim \mathcal{N}(0, \sigma_{\mathrm{RU}_k}^2)$ denotes the additive white Gaussian noise in the channel link RU_k, and $\sigma_{\mathrm{RU}_k}^2$ is the corresponding noise power. Multiuser interference caused by NOMA in (7) severely complicates the analysis of the system outage performance.

III. PERFORMANCE ANALYSIS

In this section, distribution function of the VLC channel and the system OP expression are derived.

A. Distribution Function of the VLC Channel

In order to effectively characterize the relay LED-PD performance of the relay-aided VLC system with NOMA, we use statistical channel sate information (CSI) instead of instantaneous CSI for the OP analysis. It can be seen from (1) that the distance between the LED transmitter and the PD receiver has directly impact on the VLC channel gain. Thus, the channel gain can be rewritten as [22]

$$h_\Omega = \frac{\mathrm{C}_\Omega}{(r_\Omega^2 + H_\Omega^2)^{\frac{m+3}{2}}}, \tag{8}$$

where variable $\mathrm{C}_\Omega = [(m+1)A_\Omega R_{\mathrm{PD}} g(\varphi) T(\varphi) H_\Omega^{m+1}]/(2\pi)$, $H_{\mathrm{SR}} = H_{\mathrm{S}} - H_{\mathrm{R}}$, $H_{\mathrm{RU}_k} = H_{\mathrm{R}}$, $r_{\mathrm{SR}} = r_{\mathrm{R}}$ and $r_{\mathrm{RU}_k} = r_{\mathrm{U}_k}$. Evidently, h_Ω is a monotonic decreasing function with respect to r_Ω. Based on the uniform distribution of cell-edge users, the PDF of the variable r_Ω can be given as $f_{r_\Omega}(r) = 2r/r_{\Omega\mathrm{m}}^2$, where $r_{\Omega\mathrm{m}}$ represents the maximum cell radius of source LED and relay LED-PD. Specifically, $r_{\Omega\mathrm{m}} = r_{\mathrm{c}}$ for h_{SR}^2 and $r_{\Omega\mathrm{m}} = r_{\mathrm{e}}$ for $h_{\mathrm{RU}_k}^2$, respectively. Subsequently, the PDF of the unordered variable h_Ω^2 can be given as

$$f_{h_\Omega^2}(\tau_\Omega) = \frac{1}{r_{\Omega\mathrm{m}}^2} \frac{\mathrm{C}_\Omega^{\frac{2}{m+3}}}{m+3} \tau_\Omega^{-\frac{1}{m+3}-1}, \tag{9}$$

where variable $\tau_\Omega \in [\tau_{\Omega,\mathrm{min}}, \tau_{\Omega,\mathrm{max}}]$. The upper and lower limits of τ_{SR} are given as $\tau_{\mathrm{SR,min}} = \mathrm{C}_{\mathrm{SR}}^2/(r_{\mathrm{c}}^2 + H_{\mathrm{SR}}^2)^{(m+3)}$ and $\tau_{\mathrm{SR,max}} = \mathrm{C}_{\mathrm{SR}}^2/H_{\mathrm{SR}}^{2(m+3)}$. The upper and lower limits of τ_{RU_k} are given as $\tau_{\mathrm{RU}_k,\mathrm{min}} = \mathrm{C}_{\mathrm{RU}_k}^2/(r_{\mathrm{e}}^2 + H_{\mathrm{RU}_k}^2)^{(m+3)}$ and $\tau_{\mathrm{RU}_k,\mathrm{max}} = \mathrm{C}_{\mathrm{RU}_k}^2/H_{\mathrm{RU}_k}^{2(m+3)}$. Thus, the corresponding CDF of

the unordered variable h_{SR}^2 and $h_{\text{RU}_k}^2$ can be given as

$$F_{h_{\text{SR}}^2}(\tau_{\text{SR}}) = -\frac{\text{C}_{\text{SR}}^{\frac{2}{m+3}}}{r_{\text{c}}^2}\tau_{\text{SR}}^{-\frac{1}{m+3}} + \frac{H_{\text{SR}}^2}{r_{\text{c}}^2} + 1, \qquad (10a)$$

$$F_{h_{\text{RU}_k}^2}(\tau_{\text{RU}_k}) = -\frac{\text{C}_{\text{RU}_k}^{\frac{2}{m+3}}}{r_{\text{e}}^2}\tau_{\text{RU}_k}^{-\frac{1}{m+3}} + \frac{H_{\text{RU}_k}^2}{r_{\text{e}}^2} + 1. \qquad (10b)$$

Finally, based on the order statistics knowledge in [33], the PDF of the ordered variable h_Ω^2 can be obtained as

$$f_{h_\Omega^2}^{\text{O}} = \frac{K!}{(k-1)!\,(K-k)!}\left(F_{h_\Omega^2}(t)\right)^{(k-1)}\left(1-F_{h_\Omega^2}(t)\right)^{(K-k)}f_{h_\Omega^2}(t). \qquad (11)$$

where superscript O represents the order variable. By integrating (11), the CDF of the order variable h_{SR}^2 and $h_{\text{RU}_k}^2$ can be achieved as

$$F_{h_{\text{SR}}^2}^{\text{O}}(\tau_{\text{SR}}) = -\frac{\text{C}_{\text{SR}}^{\frac{2}{m+3}}}{r_{\text{c}}^2}\tau_{\text{SR}}^{-\frac{1}{m+3}} + \frac{H_{\text{SR}}^2}{r_{\text{c}}^2} + 1, \qquad (12a)$$

$$F_{h_{\text{RU}_k}^2}^{\text{O}}(\tau_{\text{RU}_k}) = \sum_{i=k}^{K}\binom{K}{i}\left(-\frac{\text{C}_{\text{RU}_k}^{\frac{2}{m+3}}}{r_{\text{e}}^2}\tau_{\text{RU}_k}^{-\frac{1}{m+3}} + \frac{H_{\text{RU}_k}^2}{r_{\text{e}}^2} + 1\right)^{i}$$
$$\times\left(\frac{\text{C}_{\text{RU}_k}^{\frac{2}{m+3}}}{r_{\text{e}}^2}\tau_{\text{RU}_k}^{-\frac{1}{m+3}} - \frac{H_{\text{RU}_k}^2}{r_{\text{e}}^2}\right)^{K-i}, \qquad (12b)$$

where $\binom{K}{i} = \frac{K!}{i!(K-i)!}$.

B. Closed-Form OP Expression

Due to the transmission signal is subject to the constraints on the peak amplitude and average power in the practical VLC system, the traditional Shannon capacity cannot directly be applied to VLC systems [15], [34]. Moreover, it is difficult to obtain a closed-form channel capacity expression for VLC systems [35]. As a result, the tight upper bound and lower bound expressions for the achievable rate of NOMA-based VLC systems were derived in [34]. Thus, to achieve a tractable analysis expression of the OP, the lower bound of the achievable rate is adopted and then the corresponding achievable rate of the k-th user at the relay LED-PD is given as

$$R_{\text{SR},k} = \frac{1}{2}\log_2\frac{1+\mathcal{A}^2 h_{\text{SR}}^2\tilde{\alpha}_i\rho_{\text{SR}}\mu}{1+\mathcal{A}^2 h_{\text{SR}}^2\tilde{\alpha}_{i+1}\rho_{\text{SR}}}, \qquad (13)$$

where $\mu = \exp(1+2(\gamma+\varrho))/(2\pi)$, γ and ϱ can be calculated based on the equation given in [34]. ρ_{SR} represents source LED transmit SNR in the channel link SR, and it is calculated by $\rho_{\text{SR}} = P_{\text{ST}}/\sigma_{\text{SR}}^2$. Note that $\tilde{\alpha}_i = \sum_{i=k}^{K}\alpha_i$ and $\tilde{\alpha}_{K+1} = 0$.

For user terminals, the k-th user can decode the signal component of the l-th, $(\forall l < k)$ user. Thus, the achievable rate at the k-th user to detect the signal s_l is given by

$$R_{\text{RU}_{k,l}} = \frac{1}{2}\log_2\frac{1+\mathcal{A}^2 h_{\text{RU}_k}^2\tilde{\beta}_l\rho_{\text{RU}_k}\mu}{1+\mathcal{A}^2 h_{\text{RU}_k}^2\tilde{\beta}_{l+1}\rho_{\text{RU}_k}}, \qquad (14)$$

where ρ_{RU_k} represents relay LED-PD transmit SNR in the channel link RU_k, and it is calculated by $\rho_{\text{RU}_k} = P_{\text{RT}}/\sigma_{\text{RU}_k}^2$. Note that $\tilde{\beta}_l = \sum_{l=k-1}^{K}\beta_l$ and $\tilde{\beta}_{K+1} = 0$. In order to guarantee

QoS of the desired users, both relay LED-PD and the k-th user must decode correctly the desired signal, otherwise, the system occurs outage. Namely, the achievable rates of the k-th user should be satisfied to $R_{\text{SR},k} \geq R_{\text{th},k}$ and $R_{\text{RU}_{k,l}} \geq R_{\text{th},l}$, where $R_{\text{th},k}$ and $R_{\text{th},l}$ denote target rate threshold of the signal s_k and s_l, respectively. Thus, based on (13) and (14), the OP of the k-th user can be formulated as

$$P_k^{\text{DF}} = 1 - \mathbb{P}\left(R_{\text{SR},k} \geq R_{\text{th},k}\right)\mathbb{P}\left(R_{\text{RU}_{k,l}} \geq R_{\text{th},l}\right)$$
$$= 1 - \mathbb{P}\left(h_{\text{SR}}^2 \geq \underbrace{\frac{\lambda_k - 1}{\mathcal{A}^2\rho_{\text{SR}}\left(\mu\tilde{\alpha}_i - \lambda_k\tilde{\alpha}_{i+1}\right)}}_{\varepsilon_k}\right)$$
$$\times \mathbb{P}\left(h_{\text{RU}_k}^2 \geq \underbrace{\frac{\lambda_l - 1}{\mathcal{A}^2\rho_{\text{RU}_k}\left(\mu\tilde{\beta}_l - \lambda_l\tilde{\beta}_{l+1}\right)}}_{\eta_l}\right), \qquad (15)$$

where $i \leq k$, $l \leq k$. The superscript DF represents the proposed DF relay-aided VLC system with NOMA, which is simplified as DF relaying system. $\mathbb{P}[\cdot]$ is the probability of event and $\lambda_k = 2^{2R_{\text{th},k}}$, $\lambda_l = 2^{2R_{\text{th},l}}$. The OP can be obtained based on the conditions of $\mu\tilde{\alpha}_i > \lambda_i\tilde{\alpha}_{i+1}$ and $\mu\tilde{\beta}_l > \lambda_l\tilde{\beta}_{l+1}$. To simplify, two new thresholds are defined, namely, $\varepsilon_k^* = \min\{\max\{\varepsilon_1,\ldots,\varepsilon_k,\tau_{\text{SR,min}}\},\tau_{\text{SR,max}}\}$ and $\eta_l^* = \min\{\max\{\eta_1,\ldots,\eta_l,\tau_{\text{RU}_k,\text{min}}\},\tau_{\text{RU}_k,\text{max}}\}$. According to (12) and (15), the closed-form OP expression of the k-th user in the DF relaying system can be obtained as

$$P_k^{\text{DF}} = 1 - \mathbb{P}\left(h_{\text{SR}}^2 \geq \varepsilon_k^*\right)\mathbb{P}\left(h_{\text{RU}_k}^2 \geq \eta_l^*\right)$$
$$= 1 - \left(\frac{\text{C}_{\text{SR}}^{\frac{2}{m+3}}}{r_{\text{c}}^2}(\varepsilon_k^*)^{-\frac{1}{m+3}} - \frac{H_{\text{SR}}^2}{r_{\text{c}}^2}\right)$$
$$\times\left[1 - \sum_{i=k}^{K}\binom{K}{i}\times\left(\frac{H_{\text{RU}_k}^2}{r_{\text{e}}^2} - \frac{\text{C}_{\text{RU}_k}^{\frac{2}{m+3}}}{r_{\text{e}}^2}(\eta_l^*)^{-\frac{1}{m+3}} + 1\right)^{i}\right.$$
$$\left.\times\left(\frac{\text{C}_{\text{RU}_k}^{\frac{2}{m+3}}}{r_{\text{e}}^2}(\eta_l^*)^{-\frac{1}{m+3}} - \frac{H_{\text{RU}_k}^2}{r_{\text{e}}^2}\right)^{K-i}\right]. \qquad (16)$$

For comparison, a DT NOMA VLC system is assumed as a baseline scheme and is simplified as the DT system in this paper. Specifically, the cell-edge users directly communicate with source LED without a relay in the DT system. Moreover, it is assumed that the channel gain follows the order with $h_{\text{SU}_1} \leq \cdots \leq h_{\text{SU}_k} \leq \cdots \leq h_{\text{SU}_K}$ in the DT system. Similar to (16), the closed-form OP expression of the k-th user in the DT system can be given as

$$P_k^{\text{DT}} = 1 - \mathbb{P}\left(h_{\text{SU}_k}^2 \geq \zeta_k^*\right)$$
$$= \sum_{i=k}^{K}\binom{K}{i}\left(\frac{H_{\text{SU}_k}^2}{r_{\text{c}}^2} - \frac{\text{C}_{\text{SU}_k}^{\frac{2}{m+3}}}{r_{\text{c}}^2}(\zeta_k^*)^{-\frac{1}{m+3}} + 1\right)^{i}$$
$$\times\left(\frac{\text{C}_{\text{SU}_k}^{\frac{2}{m+3}}}{r_{\text{c}}^2}(\zeta_k^*)^{-\frac{1}{m+3}} - \frac{H_{\text{SU}_k}^2}{r_{\text{c}}^2}\right)^{K-i}, \qquad (17)$$

TABLE I
SIMULATION PARAMETERS

Parameter name and symbol		Value
Source transmit power	P_{ST}	2W
Peak amplitude of signal	$\mathcal{A}$	2V
DC bias offset	I_{DC}	$\sqrt{6}$A
Linear current	$[I_{\text{L}}, I_{\text{H}}]$	$[0, 5]$A
Source height	H_{S}	3.5m
Source radiation radius	r_{c}	2.5m
Relay transmit SNR	ρ_{RU_k}	$[90, 110]$dB
relay height	H_{R}	2.0m
Horizonal distance from relay to source	r_{R}	1.5m
relay radiation radius	r_{e}	1.0m
LED emission semi-angle	$\phi_{1/2}$	60^0
Receiver FoV	Ψ	60^0
PD detection area	A_Ω	1cm^2
PD responsivity	R_{PD}	0.54A/W
Refractive index	n	1.5
Optical filter gain	$T(\varphi)$	1
Noise power	σ_Ω^2	-98.82dBm

where superscript DT denotes the DT system. Subscript SU_k denotes the channel link between source LED and the cell-edge user in the DT system. $\zeta_k^* = \min\{\max\{\zeta_1, \ldots, \zeta_k, \tau_{\text{SU}_k,\min}\}, \tau_{\text{SU}_k,\max}\}$, where $\zeta_k = (\lambda_k - 1)/[\mathcal{A}^2 \rho_{\text{SU}_k}(\mu\tilde{\alpha}_i - \lambda_i\tilde{\alpha}_{i+1})]$, $\tau_{\text{SU}_k,\min} = \text{C}_{\text{SU}_k}^2/(r_{\text{c}}^2 + H_{\text{SU}_k}^2)^{(m+3)}$ and $\tau_{\text{SU}_k,\max} = \text{C}_{\text{SU}_k}^2/H_{\text{SU}_k}^{2(m+3)}$. ρ_{SU_k} denotes the source LED transmit SNR in the channel link SU_k, and it can be calculated by $\rho_{\text{SU}_k} = P_{\text{ST}}/\sigma_{\text{SU}_k}^2$.

IV. SIMULATION RESULTS AND DISCUSSION

In this section, numerical simulation results are presented to validate the accuracy of the derived theoretical expression and evaluate the effectiveness of the DF relay-aided VLC system with NOMA in improving the system outage performance. Moreover, the impact factors of the OP are analyzed from relay LED-PD transmit semi-angle, relay LED-PD deployment height, relay LED-PD radiation radius and power allocation coefficient. To simplify, in the simulation result legend, the DF relaying system and DT system are simply written as DF and DT, respectively. Simulation and theoretical analysis result curves are simplified as sim and ana, respectively.

In the simulation, the corresponding parameters settings are as follows. It is assumed that there are a source LED, a relay LED-PD and three desired cell-edge users ($K = 3$) in the considered relaying system. In the three-user scenario, the power allocation factors of source LED and relay LED-PD are respectively set as $\alpha = [0.65, 0.30, 0.05]$ and $\beta = [0.65, 0.25, 0.10]$, and the target rate thresholds of three users are all set as 0.55bits/s/Hz. Similar to the work in [34] and if not specified, the parameters used for the simulation setup are summarized in Table I.

Fig. 2 shows the system OP versus transmit SNR in the three-user scenario for the DF relaying system and the DT system, respectively. Note that, for comparing the OP with the DT system, the power allocation factors from the source LED and the relay LED-PD are set as the same value, namely, $\alpha = \beta = [0.65, 0.25, 0.10]$. It can be observed that the theoretical analysis results of the system OP are consistent with the simulation results in both the DF relaying system and the DT system. It verifies
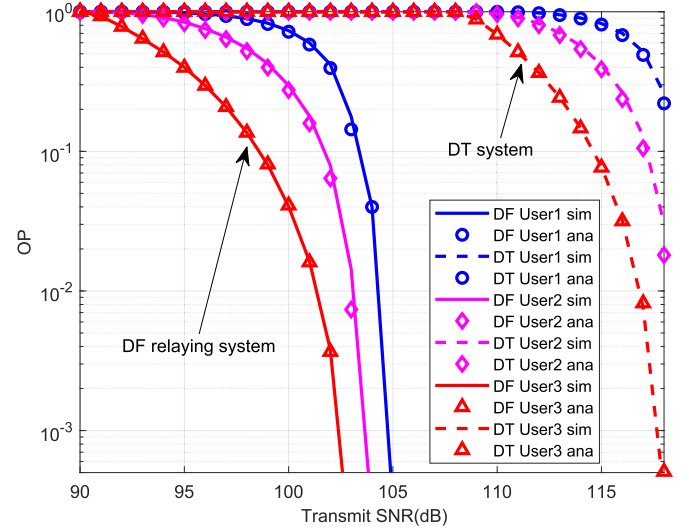

Fig. 2. System OP versus transmit SNR for the DF relaying system and the DT system with $\alpha = \beta = [0.65, 0.25, 0.10]$.
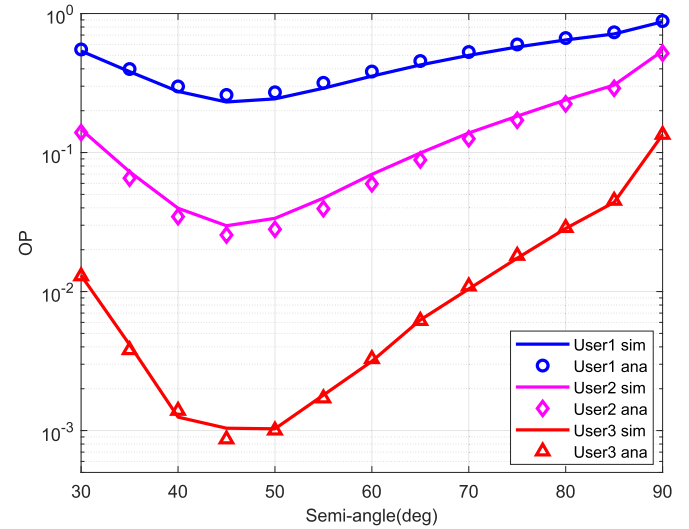

Fig. 3. System OP versus relay LED-PD transmit semi-angles in DF relaying system with $\rho_{\text{RU}_k} = 102$ dB.

the accuracy of the derived theoretical expression. Moreover, the OPs of three users follow the order of $\text{P}_3^{\text{DF}} < \text{P}_2^{\text{DF}} < \text{P}_1^{\text{DF}}$ for the DF relaying system and $\text{P}_3^{\text{DT}} < \text{P}_2^{\text{DT}} < \text{P}_1^{\text{DT}}$ for the DT system, respectively. This is owing to the channel gains of three users with $h_{\text{RU}_3} > h_{\text{RU}_2} > h_{\text{RU}_1}$ and $h_{\text{SU}_3} > h_{\text{SU}_2} > h_{\text{SU}_1}$, respectively. The system OP decreases with transmit SNR increase, because the achievable rate of the k-th user increases with the transmit SNR. More importantly, the DF relaying system can obtain 15 dB transmission SNR gains in 10^{-3} OP level over the DT system. It demonstrates that relay LED-PD can effectively improve the system outage performance. In other words, the channel transmission quality between the source transmitter and the target receiver is improved.

Fig. 3 shows the system OP versus relay LED-PD transmit semi-angles in the DF relaying system with $\rho_{\text{RU}_k} = 102$ dB.
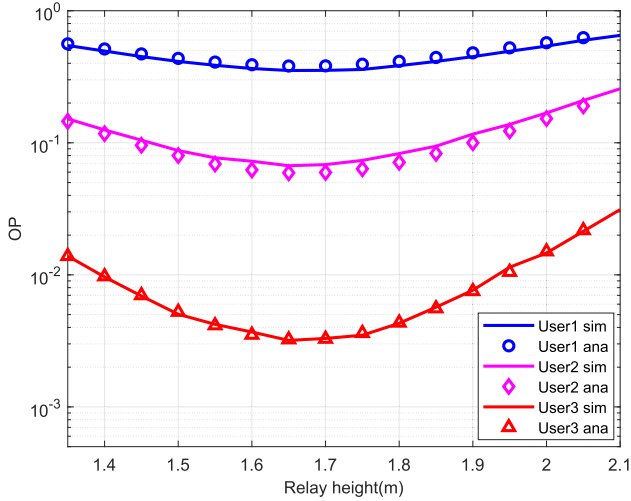
Fig. 4. System OP versus relay LED-PD deployment height in the DF relaying system with $\rho_{\mathrm{RU}_k} = 102\,\mathrm{dB}$.

Fig. 5. System OP versus relay LED-PD radiation radius in the DF relaying system with $\rho_{\mathrm{RU}_k} = 102\,\mathrm{dB}$.

It can be seen that the system OP firstly decreases and then increases with the increased relay LED-PD transmit semi-angle. It can be concluded that there is an optimal relay LED-PD semi-angle to achieve the optimal system outage performance. During the decreasing phase of the OP, the cell-edge users can obtain more LoS link light of the relay LED-PD with the increased relay LED-PD transmit semi-angle, and the corresponding channel gain is improved. However, the LoS link light from relay LED-PD is become more divergent with the further increase of relay LED-PD transmit semi-angle, then the light energy obtained by the user's PD will be reduced and the channel quality becomes poor. Thus, an optimal relay LED-PD transmit semi-angle should be chosen to improve the system outage performance in the cooperative relay LED-PD design.

Fig. 4 shows the system OP versus relay LED-PD deployment height in the DF relaying system with $\rho_{\mathrm{RU}_k} = 102\,\mathrm{dB}$. It can be observed that the system OP firstly decreases and then increases with relay LED-PD deployment height. There exists an optimal relay LED-PD deployment height in achieving the minimum OP. There are mainly two reasons. On one hand, the cell-edge users can obtain more LoS link light from relay LED-PD with the increased relay LED-PD deployment height and the channel gain is improved. Note that the increment of channel gain achieved by the LoS link light from relay LED-PD can compensate for the decrease of channel gain caused by the increased distance between relay LED-PD and the cell-edge users. On the other hand, with the further increased relay LED-PD deployment height, the channel gain attenuation caused by increasing distance dominates the trend of channel gain, and the corresponding OP is increased. Thus, relay LED-PD should be designed with an optimal deployed height to enhance the forwarding capability of relay LED-PD.

Fig. 5 presents system OP versus relay LED-PD radiation radius in the DF relaying system with $\rho_{\mathrm{RU}_k} = 102\,\mathrm{dB}$. It can be seen that the system OP increases with the relay LED-PD radiation radius. The main reason is that the probability that the user is farther away from relay LED-PD increases with relay
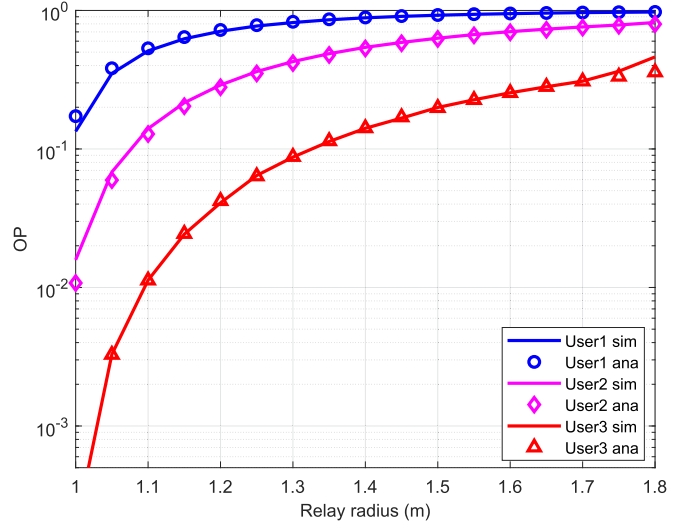
LED-PD radiation radius, and the OP in the considered scenario increases.

Fig. 6 shows system OP versus power allocation coefficient α_1 of the far user from the source LED and power allocation coefficient β_1 of the far user from the relay LED-PD in the two-user scenario. Note that a two-user scenario is considered for focusing on the impact of the power allocation factors on the OP. In the two-user scenario, power allocation coefficients of the far user U_1 and the near user U_2 are set as α_1, α_2 at the source LED and β_1, β_2 at the relay LED-PD, respectively, i.e., $\alpha = [\alpha_1, \alpha_2]$, $\beta = [\beta_1, \beta_2]$.

Fig. 6(a) shows system OP versus power allocation coefficient α_1 of far user from the source for DF relaying system with $\beta = [0.70, 0.30]$, $\rho_{\mathrm{RU}_k} = 100\,\mathrm{dB}$ and $R_{\mathrm{th},k} = 0.55\,\mathrm{bits/s/Hz}$. Note that when $0 \leq \alpha_1 < 0.6$, the far user occurs outage in the channel link SR. When $\alpha_1 = 1$, both the far user and the near user occur outage in the channel link SR. Thus, $\alpha_1 \in [0.6, 0.95]$ is considered. It can been seen from Fig. 6(a) that when $\alpha_1 \in [0.6, 0.95]$, namely, the channel link SR is connected, the power allocation coefficient α of the source LED has no impact on the system OP. This is mainly because the relay LED-PD decodes signal and then reconstructs the signal by employing power allocation coefficient β after receiving the transmitted signal by source LED.

Fig. 6(b) shows system OP versus power allocation coefficient β_1 of far user from the relay for DF relaying system with $\rho_{\mathrm{RU}_k} = 95\,\mathrm{dB}$ and $\rho_{\mathrm{RU}_k} = 100\,\mathrm{dB}$ in the two-use scenario, where the target rate threshold $R_{\mathrm{th},k} = 0.55\,\mathrm{bits/s/Hz}$. It can be observed from Fig. 6(b) that the OP of the far user decreases and the OP of the near user increases with the increased β_1. Because the achievable rates of the far user and the near user increase and decrease with β_1 increase, respectively. Moreover, it can be seen that the far user and the near user achieve the same OP when β_1 is set as a specific value. And the relay transmit SNR is higher, the system outage performance is better. It illustrates
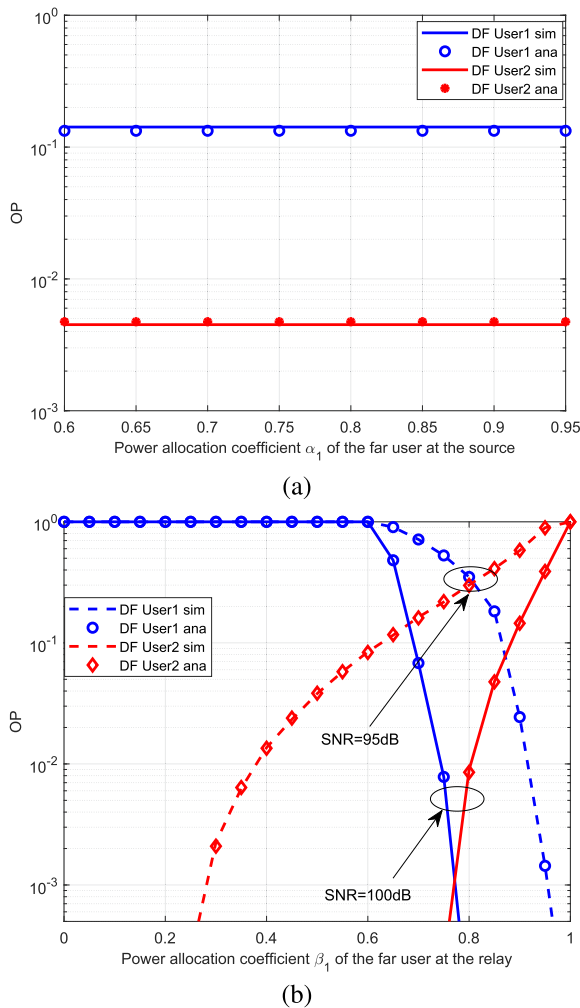
Fig. 6. System OP versus (a) power allocation coefficient α_1 of the far user from the source LED and (b) power allocation coefficient β_1 of the far user from the relay LED-PD in the two-user scenario.

that we should set reasonable power allocation coefficients and the relay transmit SNR for obtaining the optimal system outage performance.

V. CONCLUSION

In this paper, a DF relay-aided VLC system with NOMA is proposed to improve the system outage performance of the cell-edge users. Moreover, interference among NOMA users and the constraints on the peak amplitude and average power are considered in the proposed system. In order to accurately analyze the system outage performance, a statistical probability method is employed and the closed-form expression of the OP is derived. Simulation results verify the accuracy of the theoretical expression and illustrate that the proposed DF relaying system can improve the communication robustness of the cell-edge users. It can obtain 15 dB transmission SNR gains in 10^{-3} OP level compared with the DT system. Furthermore, by investigating the impact factors of the OP, the optimal relay LED-PD transmit

semi-angle and relay LED-PD deployment height are obtained to achieve the optimal system outage performance.

REFERENCES

[1] J. Liu, N. Kato, J. Ma, and N. Kadowaki, "Device-to-device communication in LTE-advanced networks: A survey," *IEEE Commun. Surv. Tut.*, vol. 17, no. 4, pp. 1923–1940, Oct.–Dec. 2015.

[2] Q. Wu, W. Chen, D. W. K. Ng, and R. Schober, "Spectral and energy efficient wireless powered IoT networks: NOMA or TDMA?," *IEEE Trans. Veh. Technol.*, vol. 67, no. 7, pp. 6663–6667, Jul. 2018.

[3] A. M. Abdelhady, O. Amin, A. Chaaban, B. Shihada, and M. S. Alouini, "Downlink resource allocation for dynamic TDMA based VLC systems," *IEEE Trans. Wireless Commun.*, vol. 18, no. 1, pp. 108–120, Jan. 2019.

[4] X. Deng, K. Arulandu, Y. Wu, G. Zhou, and J. P. M. G. Linnartz, "Performance analysis for joint illumination and visible light communication using buck driver," *IEEE Trans. Commun.*, vol. 66, no. 5, pp. 2065–2078, May 2018.

[5] L. Feng, R. Q. Hu, J. Wang, P. Xu, and Y. Qian, "Applying VLC in 5G networks: Architectures and key technologies," *IEEE Netw.*, vol. 30, no. 6, pp. 77–83, Nov./Dec. 2016.

[6] G. Pan et al., "Secure cooperative hybrid VLC-RF systems," *IEEE Trans. Wireless Commun.*, vol. 19, no. 11, pp. 7097–7107, Nov. 2020.

[7] A. M. Salhab, A. Chaaban, S. A. Zummo, and M. Alouini, "Power allocation and link selection for multicell cooperative NOMA hybrid VLC/RF systems," *IEEE Commun. Lett.*, vol. 25, no. 2, pp. 560–564, Feb. 2021.

[8] X. Zhang, Y. Zhang, Z. Yan, J. Xing, and W. Wang, "Performance analysis of cognitive relay networks over Nakagami-m fading channels," *IEEE J. Sel. Areas Commun.*, vol. 33, no. 5, pp. 865–877, May 2015.

[9] R. C. Kizilirmak, O. Narmanlioglu, and M. Uysal, "Relay-assisted OFDM-based visible light communications," *IEEE Trans. Commun.*, vol. 63, no. 10, pp. 3765–3778, Oct. 2015.

[10] L. Feng, R. Q. Hu, J. Wang, and Y. Qian, "Deployment issues and performance study in a relay-assisted indoor visible light communication system," *IEEE Syst. J.*, vol. 13, no. 1, pp. 562–670, Mar. 2019.

[11] Y. Hong, L. -K. Chen, and J. Zhao, "Channel-aware adaptive physical-layer network coding over relay-assisted OFDM-VLC networks," *J. Lightw. Technol.*, vol. 38, no. 6, pp. 1168–1177, Mar. 2020.

[12] X. Liu, Z. Chen, Y. Wang, F. Zhou, Y. Luo, and R. Q. Hu, "BER analysis of NOMA-enabled visible light communication systems with different modulations," *IEEE Trans. Veh. Technol.*, vol. 68, no. 11, pp. 10807–10821, Nov. 2019.

[13] J. Ren, X. Lei, and P. T. Mathiopoulos, "Jointly adaptive distributed beamforming and resource allocation for buffer-aided multiple-relay NOMA networks," *IEEE Trans. Commun.*, vol. 69, no. 11, pp. 7603–7617, Nov. 2021.

[14] F. Zhou, Y. Wu, Y. Liang, Z. Li, Y. Wang, and K. K. Wong, "State of the art, taxonomy, and open issues on NOMA in cognitive radio networks," *IEEE Wireless Commun.*, vol. 25, no. 2, pp. 100–108, Apr. 2018.

[15] X. Liu, Z. Chen, Y. Wang, F. Zhou, and S. Ma, "Robust artificial noise-aided beamforming for a secure MISO-NOMA visible light communication system," *China Commun.*, vol. 17, no. 11, pp. 42–53, Nov. 2020.

[16] F. Zhou, Y. Wu, R. Q. Hu, Y. Wang, and K. K. Wong, "Energy-efficient NOMA enabled heterogeneous cloud radio access networks," *IEEE Netw.*, vol. 32, no. 2, pp. 152–160, Mar. 2018.

[17] Z. Wei, L. Yang, D. W. K. Ng, J. Yuan, and L. Hanzo, "On the performance gain of NOMA over OMA in uplink communication systems," *IEEE Trans. Commun.*, vol. 68, no. 1, pp. 536–568, Jan. 2020.

[18] Z. Ding, M. Peng, and H. V. Poor, "Cooperative non-orthogonal multiple access in 5G systems," *IEEE Commun. Lett.*, vol. 19, no. 8, pp. 1462–1465, Aug. 2015.

[19] P. Xu and K. Cumanan, "Optimal power allocation scheme for non-orthogonal multiple access with α-fairness," *IEEE J. Sel. Areas Commun.*, vol. 35, no. 10, pp. 2357–2369, Oct. 2017.

[20] S. Al-Ahmadi, "On the achievable max-min rates of cooperative power-domain NOMA systems," *IEEE Access*, vol. 8, pp. 173112–173122, 2020.

[21] R. Raj and A. Dixit, "Outage analysis and reliability enhancement of hybrid VLC-RF networks using cooperative non-orthogonal multiple access," *IEEE Trans. Netw. Service Manage.*, vol. 18, no. 4, pp. 4685–4696, Dec. 2021.

[22] L. Yin, W. O. Popoola, X. Wu, and H. Haas, "Performance evaluation of non-orthogonal multiple access in visible light communication," *IEEE Trans. Commun.*, vol. 64, no. 12, pp. 5162–5175, Dec. 2016.

[23] H. Sadat, M. Abaza, S. M. Gasser, and H. ElBadawy, "Performance analysis of cooperative non-orthogonal multiple access in visible light communication," *Appl. Sci.*, vol. 9, no. 19, Sep. 2019, Art. no. 4004.

[24] Y. Xiao, P. D. Diamantoulakis, Z. Fang, Z. Ma, L. Hao, and G. K. Karagiannidis, "Hybrid lightwave/RF cooperative NOMA networks," *IEEE Trans. Wireless Commun.*, vol. 19, no. 2, pp. 1154–1166, Feb. 2020.

[25] Y. Xiao, P. D. Diamantoulakis, Z. Fang, L. Hao, Z. Ma, and G. K. Karagiannidis, "Cooperative hybrid VLC/RF systems with SLIPT," *IEEE Trans. Commun.*, vol. 69, no. 4, pp. 2532–2545, Apr. 2021.

[26] C. Zhang, J. Ye, G. Pan, and Z. Ding, "Cooperative hybrid VLC-RF systems with spatially random terminals," *IEEE Trans. Commun.*, vol. 66, no. 12, pp. 6396–6408, Dec. 2018.

[27] J. Wang, Q. Hu, J. Wang, M. Chen, and J. Wang, "Tight bounds on channel capacity for dimmable visible light communications," *J. Lightw. Technol.*, vol. 31, no. 23, pp. 3771–3779, Dec. 2013.

[28] D. Wan, M. Wen, F. Ji, Y. Liu, and Y. Huang, "Cooperative NOMA systems with partial channel state information over Nakagami-m fading channels," *IEEE Trans. Commun.*, vol. 66, no. 3, pp. 947–958, Mar. 2018.

[29] A. Arafa, E. Panayirci, and H. V. Poor, "Relay-aided secure broadcasting for visible light communications," *IEEE Trans. Commun.*, vol. 67, no. 6, pp. 4227–4239, Jun. 2019.

[30] L. Feng, H. Yang, R. Q. Hu, and J. Wang, "MmWave and VLC-based indoor channel models in 5G wireless networks," *IEEE Wireless Commun.*, vol. 25, no. 5, pp. 70–77, Oct. 2018.

[31] Y. Guo, K. Xiong, Y. Lu, D. Wang, and K. B. Letaief, "Achievable information rate in hybrid VLC-RF networks with lighting energy harvesting," *IEEE Trans. Wireless Commun.*, vol. 69, no. 10, pp. 6852–6864, Oct. 2021.

[32] X. Li, J. Li, and L. Li, "Performance analysis of impaired SWIPT NOMA relaying networks over imperfect Weibull channels," *IEEE Syst. J.*, vol. 14, no. 1, pp. 669–672, Mar. 2020.

[33] H. A. David and H. N. Nagaraja, *Order Statistics*, 3rd ed. Hoboken, NJ, USA: Wiley, 2003.

[34] S. Ma, Y. He, H. Li, S. Lu, F. Zhang, and S. Li, "Optimal power allocation for mobile users in non-orthogonal multiple access visible light communication networks," *IEEE Trans. Commun.*, vol. 67, no. 3, pp. 2233–2244, Mar. 2019.

[35] A. Mostafa and L. Lampe, "Physical-layer security for MISO visible light communication channels," *IEEE J. Sel. Areas Commun.*, vol. 33, no. 9, pp. 1806–1818, Sep. 2015.